



The Chiral Dirac-Hartree-Fock Approximation in QHD with Scalar Vertex Corrections

Hiroshi Uechi

Osaka Gakuin University, Suita, Japan

Email: uechi@ogu.ac.jp

How to cite this paper: Uechi, H. (2018) The Chiral Dirac-Hartree-Fock Approximation in QHD with Scalar Vertex Corrections. *Open Access Library Journal*, 5: e4739.

<https://doi.org/10.4236/oalib.1104739>

Received: June 25, 2018

Accepted: July 21, 2018

Published: July 24, 2018

Copyright © 2018 by author and Open Access Library Inc.

This work is licensed under the Creative Commons Attribution International License (CC BY 4.0).

<http://creativecommons.org/licenses/by/4.0/>



Open Access

Abstract

A self-consistent chiral Dirac-Hartree-Fock (CDHF) approximation generated by an effective model of the (σ, ω, π) quantum hadrodynamics (QHD) is extended to include Lorentz-scalar self-consistent vertex corrections. The scalar vertex corrections are constructed with self-consistency of QHD and Bethe-Salpeter equation, and the resulting vertex corrections are diagrammatically equivalent to self-consistent Hedin approximation, which is termed Hedin-Dirac-Hartree-Fock (HDHF) approximation. The effective model of the (σ, ω, π) quantum hadrodynamics maintains the requirement of thermodynamic consistency and density-functional theory (DFT) to a good approximation. The HDFT approximation is applied to properties of nuclear matter and neutron stars.

Subject Areas

Theoretical Physics

Keywords

Thermodynamic Consistency, Density Functional Theory, Feynman Diagram Approach, Lorentz-Scalar Vertex Corrections, Hedin-Dirac-Hartree-Fock Approximation

1. Introduction

The relativistic mean-field models of Quantum Hadrodynamics (QHD) have essentially provided a realistic description of bulk properties of nuclear matter, finite nuclei and finite Fermi systems [1]-[6], and astrophysical high density matter such as neutron stars [7] [8] [9] [10] [11]. The successes and difficulties of QHD have been examined by many researchers. In order to overcome difficulties, QHD has been extended to effective theories, such as the chiral QHD

(σ, π, ω) hadronic theories [12] [13] [14] [15] [16]. Historical motivations, successes and difficulties, evolutions and revolutions, reinterpretations and rebuttals are substantially reviewed and discussed in the reference [15] and chaps. 1-3 of the review book [16].

The mean-field approximations defined by replacing meson quantum fields with classical mean fields, $\hat{\sigma}_i \rightarrow \langle \sigma_i \rangle$ ($i = \sigma, \omega, \pi, \dots$), are all equivalent to the Hartree (tadpole) approximation when nonlinear interactions are correctly renormalized as effective masses of nucleons and mesons, effective coupling constants, effective sources of equations of motions [1] [7] [8] [9] [10]. The renormalization of interactions is correctly defined and numerically checked by the requirement of thermodynamic consistency, conserving approximations, or the density functional theory (DFT) [17] [18] [19] [20] [21]. Based on the argument, mean-field (Hartree) approximations should be extended to Hartree-Fock approximation, which is discussed in a relativistic Chiral Dirac-Hartree-Fock approximation denoted as CDHF [22].

Contributions of Fock-exchange terms are more important than those of the Hartree (mean-field) approximation at saturation density, while the Hartree approximation is important at high densities. We introduce Lorentz-scalar 3-point vertex corrections to CDHF approximation by assuming an effective interaction for two-body scattering amplitude, which is termed Hedin-Dirac-Hartree-Fock (HDHF) approximation. The HDHF approximation is applied to calculate properties of nuclear and neutron stars.

The Hartree-Fock energy density with scalar vertex corrections is explained in Section 2, and then, self-energies with vertex corrections and relations to dynamical variables are self-consistently defined by functional derivative of energy density in Section 3. The Bethe-Salpeter equation to determine scalar vertex corrections with the first-order effective interaction is explained in Section 4. The results of calculations for nuclear matter and neutron stars are shown in Section 5, and conclusion is in Section 6. The derivation of scalar vertex functions is discussed in detail in **Appendix A**.

2. The Energy Density and Lorentz-Scalar 3-Point Vertex Corrections, $\Gamma(\kappa^-, k, q)$

We discussed the self-consistent Chiral Dirac-Hartree-Fock (CDHF) approximation shown diagrammatically in **Figure 1** and examined that the Fock-exchange contributions are important at the saturation density of nuclear matter [22] compared to mean-field approximations [1] [7] [8] [9] [10]. Retardation effects produced by exchange terms are also important for calculations of incompressibility and symmetry energy, equation of state for high density matter.

Hence, we extend the CDHF approximation by including Lorentz-scalar vertex corrections that maintain self-consistency and thermodynamic consistency of QHD [1] [10] [11], requirements of the density functional theory [17] [18] [19] [20] [21]. The exact self-energies of many-body approximations cannot automatically

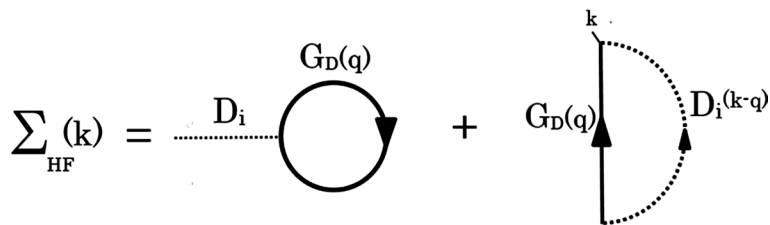


Figure 1. The Hartree-Fock self-energy drawn by propagators of baryons, $G_D(k)$, and mesons, $D_i(k)$. One should note that baryon, $G_D(k)$ (solid lines) and meson interaction lines (dotted lines), $D_i(k)$ ($i = \sigma, \pi, \omega$), are given by effective masses of nucleons and mesons, respectively.

be constructed by Feynman diagram method, since truncations of higher order interaction processes, retardation and nonlinear interactions make self-consistency ambiguous and doubtful. The self-consistency must be examined and controlled in terms of conserving approximations when sophisticated higher order corrections are introduced [21] [25]-[31].

The chiral mean-field Lagrangian is sufficiently discussed in Refs. [12] [16] [22]. Based on the Hartree-Fock energy density, \mathcal{E}_{HF} , discussed in Ref. [22], the current energy density with vertex corrections is defined and denoted as \mathcal{E}_{HFV} :

$$\mathcal{E}_{HFV} = \mathcal{E}_B + \mathcal{E}_H(\sigma, \omega) + \mathcal{E}_{FV}(\sigma, \omega, \pi) \tag{1}$$

where $\mathcal{E}_B(k_F)$, $\mathcal{E}_H(\sigma, \omega)$ and $\mathcal{E}_{FV}(\sigma, \omega, \pi)$ are the baryon, direct (Hartree), and Fock contributions with vertex corrections, respectively.

The baryon energy density is given by the self-consistent single particle energy of protons and neutrons (p, n):

$$\mathcal{E}_B = \sum_i n_i E(k_i) = \sum_{B=n,p} \frac{2}{(2\pi)^3} \int^{k_{FB}} d^3k E_B(k), \tag{2}$$

where n_i is the particle occupation number and k_{FB} is a baryon Fermi-momentum ($B = n, p$); $E_B(\mathbf{k})$ is the self-consistent baryon single particle energy. The baryon density is calculated in the ground state of nuclear matter ($T = 0$, zero-temperature) as:

$$\rho_B = \sum_i n_i = \frac{\zeta}{6\pi^2} k_F^3, \tag{3}$$

where ζ is the spin-isospin degeneracy factor and $\zeta = 2$ (neutron matter), $\zeta = 4$ (nuclear matter).

The Hartree energy density, $\mathcal{E}_H(\sigma, \omega)$, is,

$$\begin{aligned} \mathcal{E}_H(\sigma, \omega) = & \frac{1}{2} m_\sigma^2 \sigma^2 - \frac{g}{2M} (m_\sigma^2 - m_\pi^2) \left(\sigma - \frac{1}{2} \frac{g}{2M} \sigma^2 \right) \sigma^2 - \frac{1}{2} m_\omega^2 \omega_0^2 \\ & + \frac{g}{2M} (m_\sigma^2 - m_\pi^2) a \left(\sigma + \frac{1}{2} \frac{g}{2M} a \omega_0^2 - \frac{g}{2M} \sigma^2 \right) \omega_0^2, \end{aligned} \tag{4}$$

where the constant, $a = 2m_\omega^2/m_\pi^2$, is required in the new nuclear ground state due to symmetry-breaking mechanism [10]. The Fock energy density with vertex

corrections is

$$\begin{aligned} \mathcal{E}_{\text{FV}}(\sigma, \omega, \pi) = & \frac{1}{2\zeta} \sum_i \sum_j n_i n_j \frac{1}{E^*(k_i) E^*(q_j)} \\ & \times \left\{ g_\sigma^2 D_\sigma(\kappa^-) RI_\sigma(k_i, q_j) (k_i^{*\mu} q_{j\mu}^* + M^*(k_i) M^*(q_j)) \Gamma_\sigma(\kappa^-, k_i, q_j) \right. \\ & + 2g_\omega^2 D_\omega(\kappa^-) RI_\omega(k_i, q_j) (k_i^{*\mu} q_{j\mu}^* - 2M^*(k_i) M^*(q_j)) \Gamma_\omega(\kappa^-, k_i, q_j) \\ & \left. - (\zeta - 1) g_\pi^2 D_\pi(\kappa^-) RI_\pi(k_i, q_j) (-k_i^{*\mu} q_{j\mu}^* + M^*(k_i) M^*(q_j)) \Gamma_\pi(\kappa^-, k_i, q_j) \right\}, \end{aligned} \tag{5}$$

where $k^\mu q_\mu = k^0 q_0 - \mathbf{k} \cdot \mathbf{q}$ ($\mu = 0, 1, 2, 3$), and $\kappa^- = |\kappa^-| = |\mathbf{k}_i - \mathbf{q}_j|$. The terms $RI_\alpha(k_i, q_j)$ ($\alpha = \sigma, \omega, \pi$) are retardation and nonlinear interaction corrections:

$$RI_\alpha(k_i, q_j) = \frac{1}{2} - \left\{ V_\alpha(k_i, q_j) + [E(k_i) - E(q_j)]^2 \right\} D_\alpha(\kappa^-), \tag{6}$$

and $V_\alpha(k_i, q_j)$ ($\alpha = \sigma, \omega, \pi$) are meson nonlinear interactions produced by spontaneous symmetry breaking (see Ref. [22] for explicit expressions).

The self-consistent scalar vertex corrections are denoted as $\Gamma_\alpha(\kappa^-, k, q)$ ($\alpha = \sigma, \omega, \pi$) for sigma, omega, and pi mesons; self-energy corrections are introduced diagrammatically as shown in Figure 2, and they are defined by,

$$ig_\sigma \Gamma_\sigma(\kappa^-, k_i, q_j), \quad -ig_\omega \gamma_\mu \Gamma_\omega(\kappa^-, k_i, q_j), \quad g_\pi \gamma_5 \tau_a \Gamma_\pi(\kappa^-, k_i, q_j), \tag{7}$$

which lead to the exchange energy density (5), and θ is the angle between momentums, \mathbf{k} and \mathbf{q} .

3. Dynamical Variables, Self-Energies $\Sigma(k)$, and Vertex Corrections $\Gamma(\kappa, k, q)$

Self-energies are derived from the requirement of thermodynamic consistency: $\delta\mathcal{E}/\delta n_i = E(k_i)$ which generates relations between dynamical variables, ($M^*(k)$, $k^*(k)$, $E(k)$) and self-energies ($\Sigma^s(k), \Sigma^v(k), \Sigma^0(k)$). Although self-energies are obtained from Feynman-diagram method, they are not identical when nonlinear interactions and retardation interactions such as Fock-exchange, ring, ladder, ... corrections are included [21] [22] [23] [32] [33]. In other words, solutions produced by Feynman-diagram method break thermodynamic consistency when nonlinear interactions and retardation interactions become important.

By performing the first functional variation to \mathcal{E} with respect to n_i , one

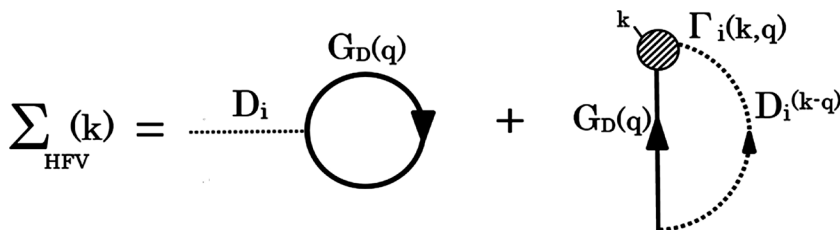


Figure 2. The scalar 3-point vertex corrections to the HF self-energy drawn by propagators of baryons, $G_D(k)$ (solid line) and mesons, $D_i(k)$ ($i = \sigma, \pi, \omega$) (dotted line).

can produce the equation for single particle energy and self-energies as:

$$\frac{\delta \mathcal{E}}{\delta n_i} = E(k_i) + \sum_j \left[\frac{\delta M^*(k_j)}{\delta n_i} \frac{\delta \mathcal{E}}{\delta M^*(k_j)} + \frac{\delta \mathbf{k}^*(k_j)}{\delta n_i} \frac{\delta \mathcal{E}}{\delta \mathbf{k}^*(k_j)} + \frac{\delta \Sigma^0(k_j)}{\delta n_i} \frac{\delta \mathcal{E}}{\delta \Sigma^0(k_j)} \right], \tag{8}$$

and by requiring the terms in the functional differential form in the right-hand side equal to 0, the self-consistent single particle energy, $E(k_i)$, is rigorously obtained, and coupled functional integro-differential equations for self-energies are generated. As specific examples, solutions from Feynman-diagram method and thermodynamic consistency are identical within Hartree and static-limit of HF approximations [23]. This is equivalent to saying that the functional derivatives of energy density with respect to $M^*(k)$, $\mathbf{k}^*(k)$, $\Sigma^0(k)$ on the right-hand side of (8) vanish by way of meson equations of motion, and one exactly obtains, $\delta \mathcal{E} / \delta n_i = E(k_i)$.

The requirement of thermodynamic consistency generates solutions identical to those derived from Feynman-diagram method, however, when retardation and nonlinear interactions are significant, solutions constructed from Feynman-diagram method become different from those constructed by (8). The requirement of thermodynamic consistency improves and produces consistent solutions compared to the solutions obtained by Feynman-diagram method. However, in general, the functional derivatives of the right-hand side of (8) do not completely vanish. One gets residual interactions connected to 3-body, 4-body, ..., N -body interactions. If self-energies are properly constructed so that thermodynamic consistency $\delta \mathcal{E} / \delta n_i = E(k_i)$ holds or is controlled, it suggests that 3-body, 4-body, ..., N -body interactions become small and correctly renormalized as quasiparticle interactions.

The Lorentz-scalar vertex functions, $\Gamma_i(\kappa^-, k, q)$, are self-consistently calculated by way of Bethe-Salpeter equations, diagrammatically depicted as **Figure 3** [34] [35]. The analytical expressions are lengthy and need some discussions to solve numerically, which are explained in **Appendix A**.

The effective mass of nucleons, $M^*(k)$, with the current scalar vertex corrections is given by

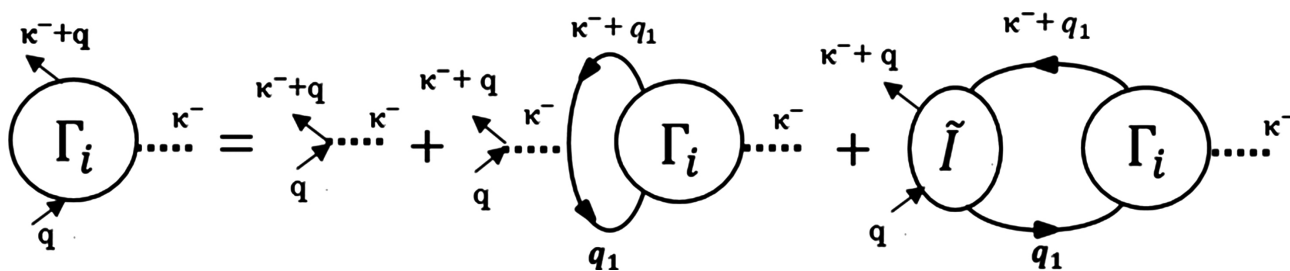


Figure 3. The Bethe-Salpeter integral equation to determine Γ_i , ($i = \sigma, \omega, \pi$). The solid lines are self-consistent Green's function, for baryons, $G_b(k)$; the wavy lines are for mesons, $D_i(k)$, and $\tilde{I}(\kappa, q, q_1)$ is the effective interactions of quasiparticles within Fermi energy, $E(k_f)$.

$$\begin{aligned}
 M^*(k_i) = & M - \frac{g_\sigma^2}{m_\sigma^2} \rho'_\sigma - \frac{1}{\zeta} \sum_j n_j \frac{M^*(q_j)}{E^*(q_j)} \left\{ g_\sigma^2 D_\sigma(\kappa^-) RI_\sigma(k_i, q_j) \right. \\
 & \times \Gamma_\sigma(\kappa^-, k_i, q_j) - 4g_\omega^2 D_\omega(\kappa^-) RI_\omega(k_i, q_j) \Gamma_\omega(\kappa^-, k_i, q_j) \\
 & \left. - (\zeta - 1) g_\pi^2 D_\pi(\kappa^-) RI_\pi(k_i, q_j) \Gamma_\pi(\kappa^-, k_i, q_j) \right\}, \tag{9}
 \end{aligned}$$

where $M^*(k_i) \rightarrow M, (k_F \rightarrow 0)$ is used, and $\kappa^- = |\kappa^-| = |\mathbf{k} - \mathbf{q}|$. The scalar density, ρ'_σ , is defined as,

$$\rho'_\sigma(k_F) = \frac{g_\sigma^2}{m_\sigma^{*2}} \left\{ \sum_i n_i \frac{M^*(k_i)}{E^*(k_i)} - \frac{m_\sigma^2 - m_\pi^2}{4M} a\omega_0^2 \right\}. \tag{10}$$

The modified momentum, $\mathbf{k}^*(k)$, is,

$$\begin{aligned}
 \mathbf{k}^*(k_i) = & \mathbf{k}_i + \frac{1}{\zeta} \frac{\mathbf{k}_i}{|\mathbf{k}_i|} \cdot \sum_j n_j \frac{\mathbf{q}^*(q_j)}{E^*(q_j)} \left\{ g_\sigma^2 D_\sigma(\kappa^-) RI_\sigma(k_i, q_j) \right. \\
 & \times \Gamma_\sigma(\kappa^-, k_i, q_j) + 2g_\omega^2 D_\omega(\kappa^-) RI_\omega(k_i, q_j) \Gamma_\omega(\kappa^-, k_i, q_j) \\
 & \left. + (\zeta - 1) g_\pi^2 D_\pi(\kappa^-) RI_\pi(k_i, q_j) \Gamma_\pi(\kappa^-, k_i, q_j) \right\}, \tag{11}
 \end{aligned}$$

where $\mathbf{k}^*(k_i) \rightarrow \mathbf{k}_i (k_F \rightarrow 0)$ is used. The 0-component self-energy, $\Sigma^0(k)$, is:

$$\begin{aligned}
 \Sigma^0(k_i) = & -\frac{g_\omega^2}{m_\omega^{*2}} \rho_B + \frac{1}{\zeta} \sum_j n_j \left\{ g_\sigma^2 D_\sigma(\kappa^-) RI_\sigma(k_i, q_j) \Gamma_\sigma(\kappa^-, k_i, q_j) \right. \\
 & + 2g_\omega^2 D_\omega(\kappa^-) RI_\omega(k_i, q_j) \Gamma_\omega(\kappa^-, k_i, q_j) \\
 & \left. + (\zeta - 1) g_\pi^2 D_\pi(\kappa^-) RI_\pi(k_i, q_j) \Gamma_\pi(\kappa^-, k_i, q_j) \right\}. \tag{12}
 \end{aligned}$$

The meson propagators are given by,

$$D_\alpha^{-1}(k_i - q_j) = (E(k_i) - E(q_j))^2 - (\mathbf{k}_i - \mathbf{q}_j)^2 - m_\alpha^2 (|\mathbf{k}_i - \mathbf{q}_j|)^2. \quad (\alpha = \sigma, \omega, \pi) \tag{13}$$

The self-energies are then related to dynamical variables and classical fields as:

$$\begin{aligned}
 M_{\text{HFV}}^*(k) & \equiv M + \Sigma_{\text{H}}^s(k_F) + \Sigma_{\text{FV}}^s(k) = M - g_\sigma (\sigma_{\text{HFV}}^D(k_F) + \sigma_{\text{HFV}}^{\text{EX}}(k)), \\
 \mathbf{k}_{\text{HFV}}^*(k) & \equiv \mathbf{k} (1 + \Sigma_{\text{FV}}^v(k)) = \mathbf{k} (1 - g_\omega |\boldsymbol{\omega}_{\text{FV}}(k)|), \\
 \Sigma_{\text{HFV}}^0(\mathbf{k}) & = \Sigma_{\text{H}}^0(k_F) + \Sigma_{\text{FV}}^0(k) = -g_\omega (\omega_{\text{HFV}}^{0D}(k_F) + \omega_{\text{HFV}}^{0\text{EX}}(k)), \\
 k^{*0} & \equiv E^*(k) \equiv (\mathbf{k}_{\text{HFV}}^{*2}(k) + M_{\text{HFV}}^*(k)^2)^{1/2}, \\
 k^{*\mu} & \equiv k^\mu + \Sigma_{\text{HFV}}^\mu(k) = (k^0 + \Sigma_{\text{HFV}}^0(k), \mathbf{k}_{\text{HFV}}^*(k)),
 \end{aligned} \tag{14}$$

and k^0 is the self-consistent single particle energy, $E(k)$. The subscript, HFV, denotes HF with vertex corrections.

4. The Scalar Vertex Corrections, $\Gamma(\kappa^-, k_i, q_j)$, and Effective Interaction $\tilde{I}(\kappa, q, q_1)$

The calculation of scalar vertex interactions requires the effective interaction of nucleons in Fermi-sea denoted as $\tilde{I}(\kappa, q, q_1)$ which is given as the kernel for Bethe-Salpeter equation (see **Figure 4**), and the effective interactions are related

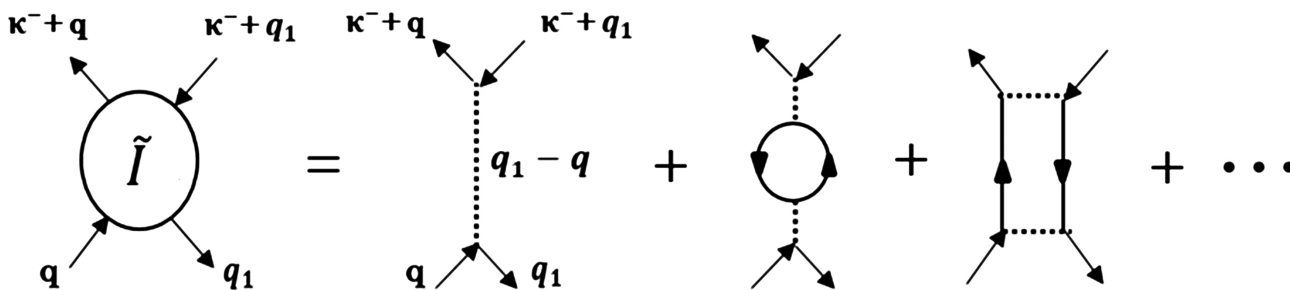


Figure 4. The diagrams for effective interactions $\tilde{I}(\kappa, q, q_1)$. Some of the first-order, lower-order interactions are only shown.

to functional derivatives of self-energy, $\Sigma(k_i)$, with respect to baryon Green's function, $G(k_j)$: $\delta\Sigma(k_i)/\delta G(k_j)$. Because Green's function is functionally connected to the particle distribution, n_i , the effective interaction can be considered equivalent to the effective two-body quasiparticle interactions: $\delta^2\mathcal{E}/\delta n_i\delta n_j = \tilde{I}(k_i, k_j)$. The effective quasiparticle interaction is given by the self-consistently renormalized nucleon and meson propagators given by $G_D(k)$ and $D_\alpha(k)$ ($\alpha = \sigma, \omega, \pi$).

As the first approximation to $\tilde{I}(\kappa, q, q_1)$, we assume the first-order diagrams of $\tilde{I}(\kappa, q, q_1)$ given by $D_\alpha(\kappa^-)$ and $D_\alpha(\xi_1^-)$ (the first diagram on the right-hand side in **Figure 4**). It results in corresponding classes of infinite partial sum of effective quasiparticle interactions. The requirement of self-consistency makes the assumption physically meaningful and controllable. It should be noted that $D_\alpha(\kappa^-)$ ($\alpha = \sigma, \omega, \pi$) is given in (13) with the single particle energy, $E(k)$, and effective masses of mesons, $m_\sigma^*(k_F, k)$, which are defined self-consistently when energy density is self-consistently determined.

The scalar vertex function by σ -meson is derived from **Figure 3**, (see, [1] [21] [22] [36]) as,

$$\Gamma_\sigma(\kappa^-, k, q) = 1 + g_\sigma^2 \int \frac{d^4q_1}{(2\pi)^4} (D_\sigma(\kappa^-) + D_\sigma(\xi_1^-)) \times \text{Tr}[G_D(q_1 + \kappa^-)G_D(q_1)]\Gamma_\sigma(\kappa^-, k, q_1), \tag{15}$$

where $\kappa^- = |\mathbf{\kappa}^-| = |\mathbf{k} - \mathbf{q}|$, $\kappa_1^- = |\mathbf{\kappa}_1^-| = |\mathbf{k} - \mathbf{q}_1|$ and $\xi_1^- = |\mathbf{\xi}_1^-| = |\mathbf{q} - \mathbf{q}_1|$. The analytical expression is given by:

$$\Gamma_\sigma(\kappa^-, k, q) = 1 + \frac{\zeta g_\sigma^2}{2} \int^{k_F} \frac{d^3q_1}{(2\pi)^3} (D_\sigma(\kappa^-) + D_\sigma(\xi_1^-)) \frac{q_1^{*\mu} \kappa_{1\mu}^{*-} + M^*(q_1)M^*(\kappa_1^-)}{E^*(q_1)E^*(\kappa_1^-)} \times \left(\frac{1}{k_0 + E(q_1) - E(\kappa_1^-) + i\epsilon} - \frac{1}{k_0 + E(\kappa_1^-) - E(q_1) - i\epsilon} \right) \Gamma_\sigma(\kappa^-, k, q_1) \Big|_{\substack{\kappa_1^- > k_F \\ k, q, q_1 < k_F}}, \tag{16}$$

where $\kappa_1^{*-} = \kappa_1^- (1 + \Sigma(\kappa_1^-))$, and $D_\sigma^{-1}(\kappa^-)$ is the σ -meson propagator given by (13).

The dynamical variables, $\mathbf{k}_\mu^*, M^*(k)$, $E^*(k)$ and $E(k)$, are defined in (14), confined within Fermi energy by $\kappa_1^- = |\mathbf{k} - \mathbf{q}_1| > k_F$, and $k, q, q_1 < k_F$. Because of

restrictions of momentums, the correction of integrations cannot be large, which is carefully checked in numerical calculations. The integrations of angles θ, θ_1 and θ_2 for vectors, $(\mathbf{k}, \mathbf{q}), (\mathbf{k}, \mathbf{q}_1), (\mathbf{q}, \mathbf{q}_1)$, and the angle φ_1 should be carefully performed as explained in an addition theorem for spherical harmonics (kq -surface is fixed for the evaluation of q_1 -integration).

One could solve (16) by iteration starting from the initial value $\Gamma_\sigma^{(0)}(\kappa^-, k, q) = 1$, until the integral equation converges. However, convergence of the integral equation depends on those of self-energies and single particle energy of the Hedin DHF approximation (HDHF), which would also depend on the selection of initial starting values. The initial starting values for the current HDHF are taken from the chiral DHF approximation [22], and convergence of calculation is defined by the difference between iteration values of single particle energies, $|E_i(k) - E_{i+1}(k)| < 10^{-8}$ (i is for an iteration number), at each Gauss-point momentum. Gauss-point integration method is used to evaluate integrations and convergences by changing the number of Gauss points. Care must be taken because momentum integrations are restricted in certain small regions of Fermi-sphere by conditions to $\kappa_1^-, \mathbf{k}, \mathbf{q}$ and \mathbf{q}_1 .

It may suggest that contributions to $\Gamma_\sigma(\kappa^-, k, q)$ from restricted momentum integrations be small, and it can be observed directly from the numerical calculation that small momentums compared to k_F do not produce contributions to the right-hand integrations of (16), and momentums close to Fermi-momentum k_F only give contributions, resulting in the scalar vertex function close to 1 in low density regions. The convergence of Hedin DHF approximation (HDHF) can be well controlled by taking initial starting values from the chiral DHF approximation.

The scalar vertex functions for ω and π mesons are similarly obtained as,

$$\begin{aligned} & \Gamma_\omega(\kappa^-, k, q) \\ &= 1 - \zeta g_\omega^2 \int^{k_F} \frac{d^3 q_1}{(2\pi)^3} (D_\omega(\kappa^-) + D_\omega(\xi_1^-)) \frac{q_1^{*\mu} \kappa_{1\mu}^{-*} - 2M^*(q_1)M^*(\kappa_1^-)}{E^*(q_1)E^*(\kappa_1^-)} \\ & \times \left(\frac{1}{k_0 + E(q_1) - E(\kappa_1^-) + i\epsilon} - \frac{1}{k_0 + E(\kappa_1^-) - E(q_1) - i\epsilon} \right) \Gamma_\omega(\kappa^-, k, q_1) \Big|_{\substack{\kappa_1^- > k_F \\ k, q, q_1 < k_F}}, \end{aligned} \tag{17}$$

and

$$\begin{aligned} & \Gamma_\pi(\kappa^-, k, q) \\ &= 1 - (\zeta - 1) g_\pi^2 \int^{k_F} \frac{d^3 q_1}{(2\pi)^3} (D_\pi(\kappa^-) + D_\pi(\xi_1^-)) \frac{-q_1^{*\mu} \kappa_{1\mu}^{-*} + M^*(q_1)M^*(\kappa_1^-)}{E^*(q_1)E^*(\kappa_1^-)} \\ & \times \left(\frac{1}{k_0 + E(q_1) - E(\kappa_1^-) + i\epsilon} - \frac{1}{k_0 + E(\kappa_1^-) - E(q_1) - i\epsilon} \right) \Gamma_\pi(\kappa^-, k, q_1) \Big|_{\substack{\kappa_1^- > k_F \\ k, q, q_1 < k_F}}. \end{aligned} \tag{18}$$

Though numerical calculations demand computing time, it is possible to evaluate the whole system of integral equations by using a modern personal com-

puter. Three vectors \mathbf{k}, \mathbf{q} and \mathbf{q}_i are in the space of 3-dimensional q_i -integration, and restrictions on momentums, addition theorem of spherical harmonics, reduction to q_i -integral equation will be explained in **Appendix A**.

5. Numerical Results for Nuclear Matter and Neutron Stars

As vertex corrections, $\Gamma_i(\kappa^-, k, q)$, are obtained as explained in sec. 3, they are employed to derive self-energies, $\Sigma^s(k), \Sigma^v(k), \Sigma^0(k)$. The convergence of calculation is defined by single particle energies, $|E_i(k) - E_{i+1}(k)| < 10^{-8}$ (i is for an iteration number), at each Gauss-point momentum as explained in sec. 4. When single particle energies do not maintain the criteria, $\Gamma_i(\kappa^-, k, q)$ calculations are repeated until $|E_i(k) - E_{i+1}(k)| < 10^{-8}$ is satisfied.

Then, the results are used to compute energy density, \mathcal{E} . However, if saturation conditions are not satisfied, the whole calculation is repeated by adjusting values of coupling constants and effective mass of sigma meson, g, g_ω, m_σ [22]. After convergences of calculations, self-consistency must be checked with the energy density. If the requirement of self-consistency is maintained, it is physically reliable, and if not, it indicates that something is not physically correct and the approximation must be rejected [26].

Self-consistency, or equivalently thermodynamic consistency in the current HDHF approximation and saturation mechanism are checked and controlled, indicating that the approximation and numerical scheme be physically and numerically acceptable (convergences in single particle energies are confirmed up to a high density $k_F \sim 2.0 \text{ fm}^{-1}$), and saturation of binding energy is shown in **Figure 5**. Therefore, the current HDHF approximation can be employed to study properties of nuclear matter and neutron stars, which are calculated with parameter values listed in **Table 1**.

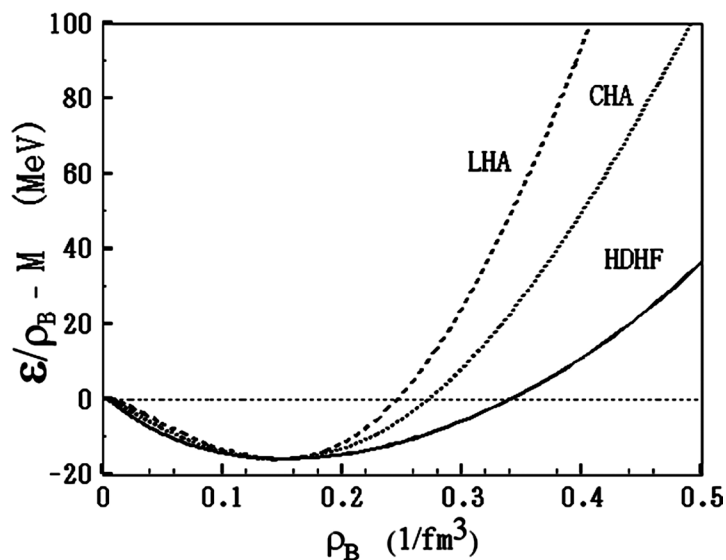


Figure 5. The binding energies of nuclear matter with LHA (linear Hartree approximation), CHA (chiral Hartree approximation) and the current Hedin-Dirac-Hartree-Fock (HDHF) approximations are shown.

Table 1. The Fermi-liquid properties of nuclear matter at saturation; the maximum mass and radius of neutron stars. The linear σ, ω mean-field approximation (LHA) [1]) and the chiral Hartree approximation (CHA) [10]) are listed for comparison. The current scalar vertex corrections is denoted as Hedin-Dirac-Hartree-Fock (HDHF) approximation [34] [35]. The parameters in the current HDHF approximation are the same as those of CDHF, $g = 1.110$, $g_\omega = 8.712$, $m_\sigma = 70.0$ MeV, $m_\omega = 783.0$ MeV, $m_\pi = 138.0$ MeV [22]. K is nuclear incompressibility at saturation density; M_{star}^{max}/M_\odot and R_{star} are the maximum mass and radius of pure neutron stars.

	M_N^*/M	m_σ^*/m_σ	m_ω^*/m_ω	m_π^*/m_π	$K(\text{MeV})$	M_{star}^{max}/M_\odot	R_{star} (km)
LHA	0.54	1	1	-	530	3.03	13.5
CHA	0.60	1.09	1.04	-	371	2.60	12.8
HDHF	0.76	1.32	1.05	1.02	218	2.22	11.6

The calculation of neutron stars requires neutron matter which should be defined by consistent nuclear matter calculation by changing isospin degrees of freedom, and therefore, thermodynamic consistency is also required for applications to high-density astronomical objects to obtain physically consistent results.

In solid state physics, scalar vertex corrections may be important [20] [34], but the scalar vertex corrections to DHF in nuclear physics are not so significant (about 1% corrections at most around saturation density), though mechanism of vertex corrections is complex. This is physically expected for the lowest-order effective-interaction corrections, because the mediator particle in QED is massless photon, whereas mediator particles for hadronic interactions are massive mesons. In addition, since the momentum integrations of vertex corrections from (16)-(18) are restricted and the first-order effective interaction in $\tilde{I}(\kappa, q, q_1)$ suppresses the momentum transfer, the scalar vertex corrections to DHF become relatively small (Figure 6 should be compared to Figure 5 in CDHF approximation [22]).

Momentum integrations of scalar vertex corrections are strictly confined and as long as energy-momentum transfers are small compared to masses of mesons, current effective-interaction corrections to the DHF approximation may not be so large, which can be observed by comparing data of the Chiral-Dirac-Hartree-Fock (CDHF) [22] and the current HDHF approximations. Even if complicated nonlinear corrections are included in a hadronic model, scalar vertex corrections are not so significant when they are self-consistently renormalized in the level of current effective interactions. The corrections from higher-order effective interactions should be investigated further based on self-consistency.

6. Conclusions

The condition of nuclear matter saturation, $\varepsilon/\rho_B - M_n = -15.75$ MeV, at the baryon density $\rho_B = 0.148 \text{ fm}^{-3}$, ($k_F = 1.30 \text{ fm}^{-1}$), must be shown at the outset, in order to obtain consistent results and conclusions in nuclear physics [26]. The theoretical meaning of saturation in many-body theory of nuclear matter has

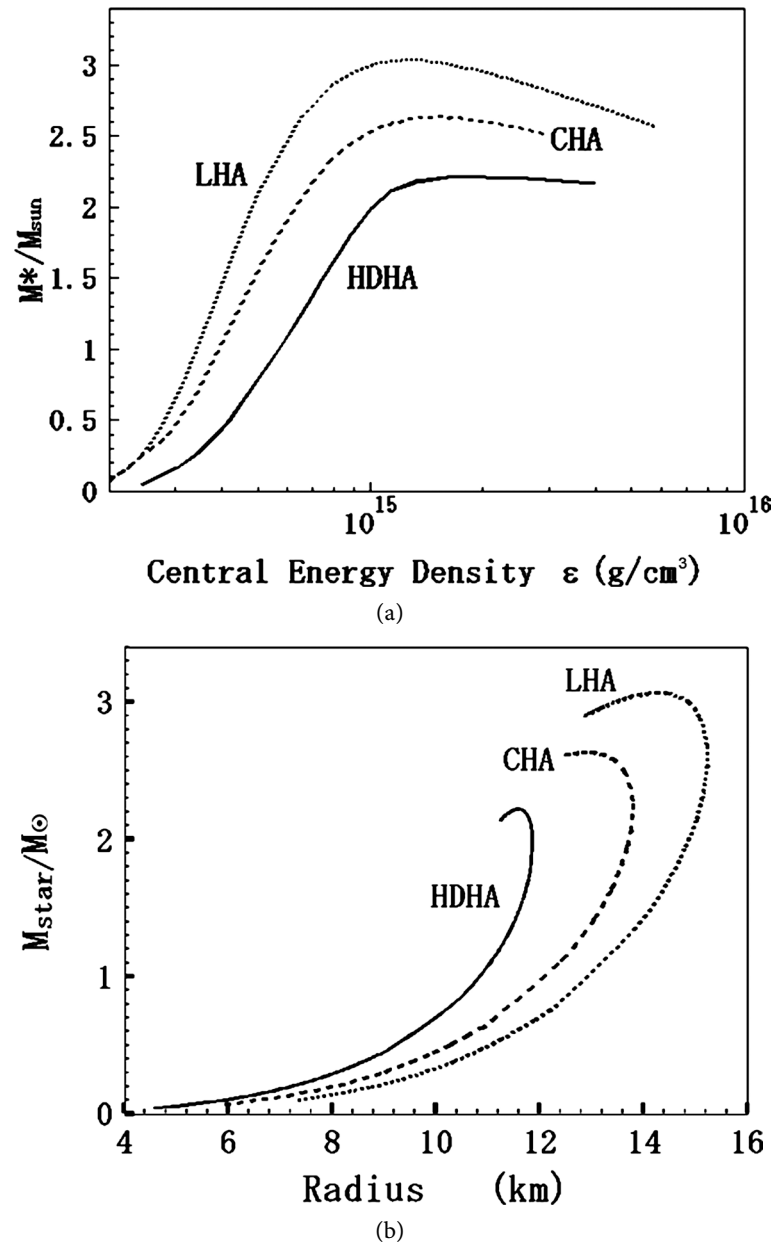


Figure 6. (a) The mass vs. central energy density of pure neutron stars; (b) The masses and radii for pure neutron stars.

been studied by many researchers, which has resulted in a useful concept as thermodynamic consistency [21] [24], conserving approximations [27] [28], and the requirement of density functional theory (DFT) [17] [18].

When numerical calculations and programmings demand considerable time to execute, one of important problems would be to show: how time-demanding numerical results are physically reliable. Self-consistency helps checking numerical accuracy and physical analysis. The saturation condition and thermodynamic consistency are not taken for granted in any models and approximations, in the cases that coupling constants and masses, complicated nonlinear and

many-body interactions, diagrammatic extensions to higher order approximations are introduced.

We investigated scalar vertex corrections by employing a class of self-consistent interaction chosen for the effective quasiparticle interaction $\tilde{I}(\kappa, q, q_1)$. Corrections to Dirac-Hartree-Fock approximation exerted from the current scalar vertex interactions are not significant in all densities. However, scalar vertex interactions exerted from higher-order classes of effective interactions should be investigated further.

The HDHF approximation will be extended by including Ring, Ladder and other classes of diagrams and electromagnetic interactions. Properties of nuclear matter and neutron stars, applications to nuclear fission [37] [38] and radiation mechanism will be investigated in the near future.

References

- [1] Serot, B.D. and Walecka, J.D. (1986) *Advances in Nuclear Physics*. Negele, J.W. and Vogt, E., Eds., Plenum, New York, Vol. 16.
- [2] Walecka, J.D. (1974) A Theory of Highly Condensed Matter. *Annals of Physics*, **83**, 491. [https://doi.org/10.1016/0003-4916\(74\)90208-5](https://doi.org/10.1016/0003-4916(74)90208-5)
- [3] Serot, B.D. (1992) Quantum Hadrodynamics. *Reports on Progress in Physics*, **55**, 1855. <https://doi.org/10.1088/0034-4885/55/11/001>
- [4] Serot, B.D. and Uechi, H. (1987) Neutron Stars in Relativistic Hadron-Quark Models. *Annals of Physics*, **179**, 272. [https://doi.org/10.1016/0003-4916\(87\)90137-0](https://doi.org/10.1016/0003-4916(87)90137-0)
- [5] Serot, B.D. and Walecka, J.D. (1992) Relativistic Nuclear Many-Body Theory. In: Ainsworth, T.L., Campbell, C.E., Clements, B.E. and Krotscheck, E., Eds., *Recent Progress in Many-Body Theories*, Vol. 3, Plenum, New York, p. 49. https://doi.org/10.1007/978-1-4615-3466-2_5
- [6] Serot, B.D. (2004) Covariant Effective Field Theory for Nuclear Structure and Nuclear Currents. *Lecture Notes in Physics*, **641**, 31. https://doi.org/10.1007/978-3-540-39911-7_2
- [7] Uechi, H. (2006) Properties of Nuclear and Neutron Matter in a Nonlinear $\sigma - \omega - \rho$ Mean-Field Approximation with Self- and Mixed-Interactions. *Nuclear Physics A*, **780**, 247. <https://doi.org/10.1016/j.nuclphysa.2006.10.015>
- [8] Uechi, H. (2008) Density-Dependent Correlations between Properties of Nuclear Matter and Neutron Stars in a Nonlinear σ, π, ω Mean-Field Approximation. *Nuclear Physics A*, **799**, 181. <https://doi.org/10.1016/j.nuclphysa.2007.11.003>
- [9] Uechi, S.T. and Uechi, H. (2015) Hardon-Quark Hybrid Stars Constructed by the Nonlinear (σ, ω, ρ) Mean-Field Model and MIT-Bag Model. *Open Access Library Journal*, **2**, e2012. <https://doi.org/10.4236/oalib.1102012>
- [10] Uechi, S.T. and Uechi, H. (2015) Density-Dependent Properties of Hadronic Matter in an Extended Chiral (σ, π, ω) Mean-Field Model. *Open Access Library Journal*, **2**, e2011. <https://doi.org/10.4236/oalib.1102011>
- [11] Uechi, S.T. and Uechi, H. (2016) Landau Theory of Fermi Liquid in a Relativistic Nonlinear (σ, ω) Model at Finite Temperature. *Open Access Library Journal*, **3**, e2757. <https://doi.org/10.4236/oalib.1102757>
- [12] Walecka, J.D. (1995) *Theoretical Nuclear and Subnuclear Physics*. Oxford University Press, Oxford.

- [13] Serot, B.D. and Walecka, J.D. (1992) Chiral QHD with Vector Mesons. *Acta Physica Polonica B*, **23**, 655.
- [14] Müller, H. and Serot, B.D. (1996) Relativistic Mean-Field Theory and the High-Density Nuclear Equation of State. *Nuclear Physics A*, **606**, 508-537. [https://doi.org/10.1016/0375-9474\(96\)00187-X](https://doi.org/10.1016/0375-9474(96)00187-X)
- [15] Furnstahl, R.J. and Serot, B.D. (2000) Comments on Nuclear Particle Physics. *Comments on Modern Physics*, **2**, 23-45.
- [16] Uechi, H., Uechi, S.T. and Serot, B.S. (2012) Neutron Stars: The Aspect of High Density Matter, Equations of State and Observables. Nova Science Publishers, New York.
- [17] Kohn, W. and Sham, L.J. (1965) Self-Consistent Equations Including Exchange and Correlation Effects. *Physical Review*, **140**, A1133-A1138. <https://doi.org/10.1103/PhysRev.140.A1133>
- [18] Kohn, W. (1999) Nobel Lecture: Electronic Structure of Matter-Wave Functions and Density Functional. *Reviews of Modern Physics*, **71**, 1253-1266. <https://doi.org/10.1103/RevModPhys.71.1253>
- [19] Aryasetiawan, F. and Gunnarsson, O. (1998) The GW Method. *Reports on Progress in Physics*, **61**, 237-312. <https://doi.org/10.1088/0034-4885/61/3/002>
- [20] Takada, Y. (2001) Self-Energy Revision Operator Theory for the Many-Body Problem: Application to Dynamical Properties of the Electron Gas. *International Journal of Modern Physics B*, **15**, 2595. <https://doi.org/10.1142/S0217979201006471>
- [21] Uechi, H. (2004) The Theory of Conserving Approximations and the Density Functional Theory in Approximations for Nuclear Matter. *Progress of Theoretical Physics*, **111**, 525. <https://doi.org/10.1143/PTP.111.525>
- [22] Uechi, S.T. and Uechi, H. (2017) Self-Consistent Many-Body Theory and Nuclear Matter in a Chiral Dirac-Hartree-Fock Approximation. *Quarterly Physics Review*, **3**, 1-19.
- [23] Uechi, H. (1989) Fermi-Liquid Properties of Nuclear Matter in a Dirac-Hartree-Fock Approximation. *Nuclear Physics A*, **501**, 813-834. [https://doi.org/10.1016/0375-9474\(89\)90162-0](https://doi.org/10.1016/0375-9474(89)90162-0)
- [24] Uechi, H. (1992) Landau Fermi-Liquid Theory and Approximations in the Quantum Hadrodynamical Model. *Nuclear Physics A*, **541**, 397-412. [https://doi.org/10.1016/0375-9474\(92\)90183-K](https://doi.org/10.1016/0375-9474(92)90183-K)
- [25] Hugenholtz, N.M. and Van Hove, L. (1958) A Theorem on the Single Particle Energy in a Fermi Gas with Interaction. *Physica*, **24**, 363-376. [https://doi.org/10.1016/S0031-8914\(58\)95281-9](https://doi.org/10.1016/S0031-8914(58)95281-9)
- [26] Day, B.D. (1978) Current State of Nuclear Matter Calculations. *Reviews of Modern Physics*, **50**, 495. <https://doi.org/10.1103/RevModPhys.50.495>
- [27] Baym, G. and Kadanoff, L.P. (1961) Conservation Laws and Correlation Functions. *Physical Review*, **124**, 287. <https://doi.org/10.1103/PhysRev.124.287>
- [28] Baym, G. (1962) Self-Consistent Approximations in Many-Body Systems. *Physical Review*, **127**, 1391-1401. <https://doi.org/10.1103/PhysRev.127.1391>
- [29] Bonitz, M., Nareyka, R. and Semkat, D. (2000) Progress in Nonequilibrium Green's Functions. World Scientific, Singapore.
- [30] Bonitz, M., Nareyka, R. and Semkat, D. (2003) Progress in Nonequilibrium Green's Functions II. World Scientific, Singapore.
- [31] Takada, Y. (1995) Exact Self-Energy of the Many-Body Problem from Conserving Approximations. *Physical Review B*, **52**, 12708-12719.

-
- <https://doi.org/10.1103/PhysRevB.52.12708>
- [32] Uechi, H. (1990) Constraints on the Self-Consistent Relativistic Fermi-Sea Particle Formalism in the Quantum Hadrodynamical Model. *Physical Review C*, **41**, 744-752. <https://doi.org/10.1103/PhysRevC.41.744>
- [33] Uechi, H. (2001) Self-Consistent Structure in a Relativistic Dirac-Hartree-Fock Approximation. *Nuclear Physics A*, **696**, 511-526. [https://doi.org/10.1016/S0375-9474\(01\)01139-3](https://doi.org/10.1016/S0375-9474(01)01139-3)
- [34] Takada, Y. (2001) Inclusion of Vertex Corrections in the Self-Consistent Calculation of Quasiparticles in Metals. *Physical Review Letters*, **87**, Article ID: 226402. <https://doi.org/10.1103/PhysRevLett.87.226402>
- [35] Hedin, L. (1965) New Method for Calculating the One-Particle Green's Function with Application to the Electron-Gas Problem. *Physical Review*, **139**, A796-A823. <https://doi.org/10.1103/PhysRev.139.A796>
- [36] Fetter, A.L. and Walecka, J.D. (2003) *Quantum Theory of Many-Particle Systems*. Dover Pub., New York.
- [37] Petkov, I.Z. and Stoitsov, M.V. (1991) *Nuclear Density Functional Theory*. Clarendon Press, Wotton-under-Edge.
- [38] Krappe, H.K. and Pomorski, K. (2012) *Theory of Nuclear Fission*. Springer, Berlin. <https://doi.org/10.1007/978-3-642-23515-3>

Appendix A. $\Gamma(\kappa, k, q)$ -Function Expressions

The scalar vertex corrections, (15)-(18), are evaluated in detail. The coordinate k_z in momentum space k is fixed by choosing the direction of momentum k as the z-coordinate: $k_z \parallel k$. The angles $(\theta, \theta_1, \theta_2; \varphi_1)$ are shown as in **Figure 7**. In order to integrate with respect to (θ_1, φ_1) variables, the kq -surface is taken as $k_x k_z$ -plain, which means that the angle φ is assumed as $\varphi \equiv 0$ when q_1 -integration is performed.

The following relation,

$$\cos \theta_2 = \cos \theta \cos \theta_1 + \sin \theta \sin \theta_1 \cos \varphi_1, \tag{A1}$$

is denoted as,

$$z_2 = z z_1 + \sqrt{(1-z^2)(1-z_1^2)} \cos \varphi_1, \tag{A2}$$

where $z = \cos \theta, z_1 = \cos \theta_1$ and $z_2 = \cos \theta_2$.

The Equations (16)-(18) are to be evaluated, and because they have a similar integration-core structure, it suffices to evaluate $\Gamma_\sigma(\kappa^-, k, q)$:

$$\begin{aligned} & \Gamma_\sigma(\kappa^-, k, q) \\ &= 1 + \frac{\zeta g_\sigma^2}{2} \int^{k_F} \frac{d^3 q_1}{(2\pi)^3} (D_\sigma(\kappa^-) + D_\sigma(\xi_1^-)) \frac{q_1^{*\mu} \kappa_{1\mu}^{*-} + M^*(q_1) M^*(\kappa_1^-)}{E^*(q_1) E^*(\kappa_1^-)} \\ & \times \left(\frac{1}{k_0 + E(q_1) - E(\kappa_1^-) + i\epsilon} - \frac{1}{k_0 + E(\kappa_1^-) - E(q_1) - i\epsilon} \right) \Gamma_\sigma(\kappa^-, k, q_1) \Big|_{\substack{\kappa_1^- > k_F \\ k, q, q_1 < k_F}}, \end{aligned} \tag{A3}$$

where $\kappa_1^- = |\mathbf{k} - \mathbf{q}_1| = (k^2 + q_1^2 - 2kq_1 z_1)^{1/2}$ and

$$\xi_1^- = |\mathbf{q} - \mathbf{q}_1| = (q^2 + q_1^2 - 2qq_1 z z_2)^{1/2}.$$

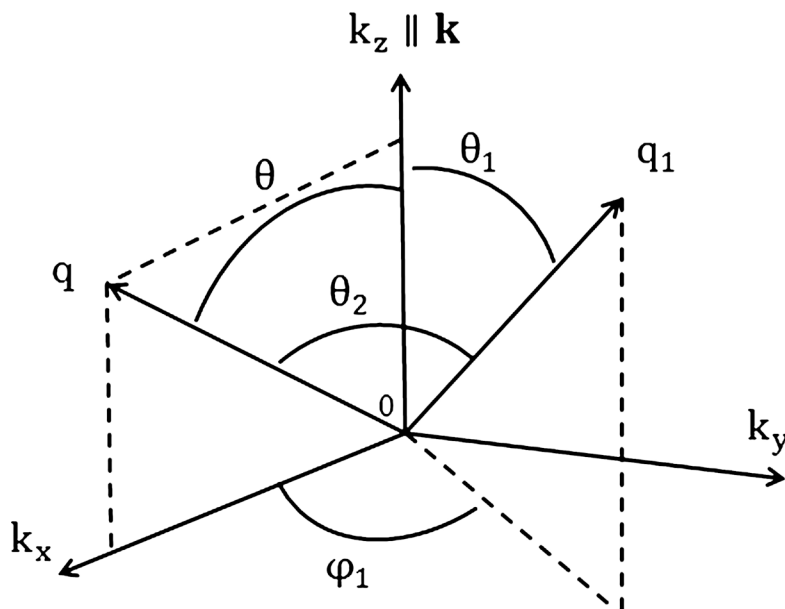


Figure 7. The coordinate k_z is fixed by: $k_z \parallel k$, and kq -surface is taken as $k_x k_z$ -plain.

The meson propagators are given by [1],

$$D_\sigma(\kappa^-) = D_\sigma(k, q, \theta) = (E(k) - E(q))^2 - (\mathbf{k} - \mathbf{q})^2 - m_i^{*2} (|k - q|)^{-1} \quad (A4)$$

$$D_\sigma(\xi_1^-) = D_\sigma(q, q_1, \theta_1, \varphi_1) = (E(q) - E(q_1))^2 - (\mathbf{q} - \mathbf{q}_1)^2 - m_i^{*2} (|q - q_1|)^{-1}. \quad (A5)$$

The propagator $D_\sigma(\xi_1^-)$ has φ -variable, which is written explicitly as,

$$D_\alpha(k, q, \theta) = \frac{1}{2kq} \frac{1}{(z - A_\alpha(k, q)/2kq)} \quad (A6)$$

$$D_\alpha(q, q_1, \varphi_1) = \frac{1}{2qq_1} \frac{1}{(zz_1 + \sqrt{(1-z^2)(1-z_1^2)} \cos \varphi_1 - A_\alpha(q, q_1)/2qq_1)}, \quad (A7)$$

where $A_\alpha(q, q_1) = q^2 + q_1^2 + m_\alpha^{*2} (|q - q_1|) - (E(q) - E(q_1))^2$, ($\alpha = \sigma, \omega, \pi$). The momentum-dependence of the effective mass is supposed as

$m_\alpha^*(|q - q_1|) \rightarrow m_\alpha^*(\| |q| - |q_1| \|)$ for numerical calculations (angle dependences of θ_1, φ_1 are neglected). The momentum dependence of $M^*(\kappa_1^-), E^*(\kappa_1^-)$ and $E(\kappa_1^-)$ should be $M^*(|\kappa_1^- - q|), E^*(|\kappa_1^- - q|)$ and $E(|\kappa_1^- - q|)$, but q -angle and momentum dependence in these terms are neglected, which may be checked numerically admissible from the fact that numerical results are compatible with thermodynamic consistency.

In order to perform φ_1 -integration, it is assumed that $\Gamma_\sigma(\kappa^-, k, q)$ does not depend on φ_1 explicitly. Hence, the term $D_\sigma(\xi_1^-)$ has only the φ_1 -dependence. The integration is performed as,

$$\int_0^{2\pi} d\varphi_1 D_\sigma(q, q_1, \varphi_1) = \frac{2\pi}{2qq_1} \frac{1}{\sqrt{B^2 - C^2}} \equiv \frac{2\pi}{2qq_1} F(z, z_1), \quad (A8)$$

with $B = zz_1 - A_\sigma(q, q_1)/2qq_1$ and $C = \sqrt{(1-z^2)(1-z_1^2)}$. The simplified form of $\Gamma_\sigma(\kappa^-, k, q)$ is obtained as:

$$\begin{aligned} & \Gamma_\sigma(\kappa^-, k, q) \\ &= 1 + \frac{\zeta g_\sigma^2}{8\pi^2} \int_0^{k_F} dq_1 q_1^2 \int_{-1}^1 dz_1 \left(D_\sigma(k, q) + \frac{F_\sigma(z, z_1)}{2qq_1} \right) \left(1 + \frac{M^*(q_1)M^*(\kappa_1^-) - \mathbf{q}_1^* \cdot \kappa_1^{*-}}{E^*(q_1)E^*(\kappa_1^-)} \right) \quad (A9) \\ & \times \left(\frac{1}{k_0 + E(q_1) - E(\kappa_1^-) + i\epsilon} - \frac{1}{k_0 + E(\kappa_1^-) - E(q_1) - i\epsilon} \right) \Gamma_\sigma(\kappa^-, k, q_1) \Big|_{\substack{\kappa_1^- > k_F \\ k, q, q_1 < k_F}}, \end{aligned}$$

and if conditions of momentums are not satisfied, the q_1 -integration will vanish, resulting in $\Gamma_\sigma(\kappa^-, k, q) = 1$. The relation:

$$\frac{1}{x \pm i\epsilon} = \mathcal{P} \frac{1}{x} \mp i\pi \delta(x), \quad (A10)$$

is used to rewrite the following term as (\mathcal{P} and $\delta(x)$ respectively stand for Cauchy's principle-value integration and the delta function),

$$\frac{1}{k_0 + E(q_1) - E(\kappa_1^-) + i\epsilon} - \frac{1}{k_0 + E(\kappa_1^-) - E(q_1) - i\epsilon} \rightarrow \frac{2W_{\kappa q}}{k_0^2 - W_{\kappa q}^2}, \quad (A11)$$

where $W_{\kappa q} = E(\kappa) - E(q)$ and $k_0 = E(k)$. We are interested in the ground

state energy of nuclear matter and so, the real part of (A11) is considered. The scalar vertex correction for σ -meson is finally written as,

$$\begin{aligned} &\Gamma_\sigma(\kappa^-, k, q) \\ &= 1 + \frac{\zeta g_\sigma^2}{8\pi^2} \int_0^{k_F} dq_1 q_1^2 \int_{-1}^1 dz_1 \left(D_\sigma(k, q) + \frac{F_\sigma(z, z_1)}{2qq_1} \right) \\ &\quad \times \left(1 + \frac{M^*(q_1)M^*(\kappa_1^-) - \mathbf{q}_1^* \cdot \boldsymbol{\kappa}_1^{*-}}{E^*(q_1)E^*(\kappa_1^-)} \right) \frac{2W_{\kappa q}}{k_0^2 - W_{\kappa q}^2} \Gamma_\sigma(\kappa^-, k, q_1) \Big|_{\substack{\kappa_1^- > k_F \\ k, q, q_1 < k_F}}. \end{aligned} \tag{A12}$$

It should be noted that $\mathbf{q}_1^* \cdot \boldsymbol{\kappa}_1^{*-} = q_1^*(kz_1 - q_1)\kappa_1^- / \kappa_1^-$.

The other ω and π scalar vertex corrections are given by:

$$\begin{aligned} &\Gamma_\omega(\kappa^-, k, q) \\ &= 1 - \frac{\zeta g_\omega^2}{4\pi^2} \int_0^{k_F} dq_1 q_1^2 \int_{-1}^1 dz_1 \left(D_\omega(k, q) + \frac{F_\omega(z, z_1)}{2qq_1} \right) \\ &\quad \times \left(1 - \frac{\mathbf{q}_1^* \cdot \boldsymbol{\kappa}_1^{*-} + 2M^*(q_1)M^*(\kappa_1^-)}{E^*(q_1)E^*(\kappa_1^-)} \right) \frac{2W_{\kappa q}}{k_0^2 - W_{\kappa q}^2} \Gamma_\omega(\kappa^-, k, q_1) \Big|_{\substack{\kappa_1^- > k_F \\ k, q, q_1 < k_F}}, \end{aligned} \tag{A13}$$

and

$$\begin{aligned} &\Gamma_\pi(\kappa^-, k, q) \\ &= 1 - \frac{(\zeta - 1)g_\pi^2}{4\pi^2} \int_0^{k_F} dq_1 q_1^2 \int_{-1}^1 dz_1 \left(D_\pi(k, q) + \frac{F_\pi(z, z_1)}{2qq_1} \right) \\ &\quad \times \left(-1 + \frac{\mathbf{q}_1^* \cdot \boldsymbol{\kappa}_1^{*-} + M^*(q_1)M^*(\kappa_1^-)}{E^*(q_1)E^*(\kappa_1^-)} \right) \frac{2W_{\kappa q}}{k_0^2 - W_{\kappa q}^2} \Gamma_\pi(\kappa^-, k, q_1) \Big|_{\substack{\kappa_1^- > k_F \\ k, q, q_1 < k_F}}. \end{aligned} \tag{A14}$$

The integral equations, (A12)-(A14), may be solved iteratively with a starting value, $\Gamma_\sigma^{(0)}(\kappa^-, k, q) = 1$. One should be careful that the time and iterations for the convergence of Γ_α depend on those of self-energies whose starting values are chosen from the result of CDHF approximation [22]. The convergence of numerical values is checked by changing Gauss-integration method.